Journal of Organometallic Chemistry 732 (2013) 109–115

Contents lists available at SciVerse ScienceDirect

Journal of Organometallic Chemistry

journal homepage: www.elsevier.com/locate/jorganchem

The C–H activation of pendant naphthyl group of 1-alkyl-2-(naphthyl-α-azo) imidazole by rhodium(III). Spectral, structural characterization and, DFT computation

Dibakar Sardar [a,1], Papia Datta [a,2], Rajat Saha [b], Pallepogu Raghavaiah [c], Chittaranjan Sinha [a,*]

[a] Department of Chemistry, Jadavpur University, Kolkata 700 032, India
[b] Department of Physics, Jadavpur University, Kolkata 700 032, India
[c] School of Chemistry, National Single Crystal X-ray Diffractometer Facility, University of Hyderabad, Hyderabad 500 046, India

ARTICLE INFO

Article history:
Received 12 November 2012
Received in revised form
4 February 2013
Accepted 12 February 2013

Keywords:
Rhodium(III) complexes
Naphthylazoimidazole
Cyclometallation
Structure
DFT computation

ABSTRACT

The reaction of $RhCl_3$ with 1-alkyl-2-(naphthyl-α-azo)imidazole (α-NaiR, *N*, *N*′chelator) (R = CH_3, CH_2 $-CH_3$, CH_2-Ph) has synthesized a coordination compound, [Rh(α-NaiR-*N*, *N*′)$(PPh_3)Cl_3$] (**2**) from boiling methanol in the presence of PPh_3 while the reaction under similar condition in the presence of Et_3N has synthesized cyclometallated complex, [Rh(α-NaiR-*N*, *N*′, C)$(PPh_3)Cl_2$] (**3**). The structures of both types of complexes are confirmed by single crystal X-ray diffraction study in representative cases. All the complexes have been characterized by spectral data (FT-IR, UV–VIS, MS, ^{1}H-NMR) and elemental analyses. Density functional theory calculation has also been performed to rationalize the electronic structures and their spectral properties.

© 2013 Elsevier B.V. All rights reserved.

1. Introduction

The azo functionalized (–N=N–) compounds are versatile dyes and pigments and have been used in the development of various types of transition metal complexes [1–8]. These complexes have exhibited different exciting properties related to electron transfer reaction, photochromism, liquid crystals, photoluminescence etc [9–20]. Some of the azo ligands are used for metal assisted organic transformation, and such type of reaction has a considerable interest because of potential application in organic synthesis and catalysis [21–25], material science [26,27], mesogens and metallomesogens [28], and biological activity [29]. A major goal of current chemical research is to achieve metal-catalysed activation of the C–H bond who could be used for the synthesis of new molecules those are otherwise difficult to synthesize or even impossible. The presence of suitable donor centre to the coordinating ligand used for metal mediated C–H activation may synthesize cyclometallated compounds (Eq. (1)).

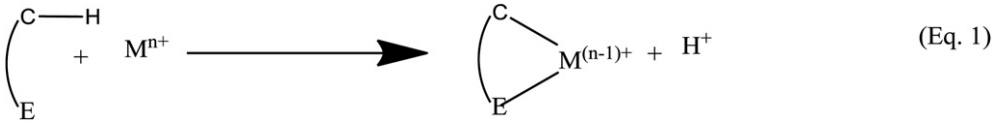

(Eq. 1)

(1).

We have been engaged for the last several years to design azo functionalized imidazoles and their derivatives such as 1-alkyl-2-(arylazo)imidazole [16]. Imidazole is very interesting molecule to chemistry and biology [30,31]. Imidazolyl group carries two N-centers of different hardness and can bridge two metal centers [32]. If we block one of the N-centers by alkyl group to synthesize 1-alkyl-2-(arylazo)imidazole then molecule may primarily serve as

* Corresponding author. Fax: +91 033 2413 7121.
E-mail address: c_r_sinha@yahoo.com (C. Sinha).
[1] Present address: Dinabandhu Andrews College, Garia, Kolkata 700084, India.
[2] Present address: RCC Institute of Information Technology, Canal South Road, Kolkata 700015, India.

0022-328X/$ – see front matter © 2013 Elsevier B.V. All rights reserved.
http://dx.doi.org/10.1016/j.jorganchem.2013.02.013

bidentate *N*–*N*′-chelator [16–20]. 1-Alkyl-2-(naphthyl-α-azo) imidazole (α-NaiR, Scheme 1) has some interesting ability to synthesise both coordination and cyclopalladated complexes [33]. The ligand, α-NaiR has two specific donor centres–*N*(imidazolyl) (*N*), *N*(azo) (*N*′), and is abbreviated as α-NaiR-*N*, *N*′; in the cyclopalladated product the C–H group *ortho* to the –*N*=*N*– function of the pendant naphthyl group serves as cyclometallation centre and is abbreviated as α-NaiR-*N*, *N*′,C. This reaction has stimulated us to synthesize organometallics of other platinum group metals. In the present work, we have characterized the complexes of Rh(III) with α-NaiR (R = CH_3, CH_2–CH_3, CH_2–Ph) (Scheme 1); the manipulation of the reaction condition has synthesized either coordination complex, [Rh(α-NaiR-*N*, *N*′)(PPh_3)Cl_3] (**2**) or the cyclometallated derivative, [Rh(α-NaiR-*N*, *N*′, C)(PPh_3)Cl_2] (**3**). The products are structurally characterized by single crystal X-ray diffraction study and the electronic spectra are explained by DFT computation of optimized geometry.

2. Experimental

2.1. Materials

$RhCl_3 \cdot 3H_2O$ was obtained from Arora-Mathy, India and used as it was received. Triphenylphosphine, triethylamine and the solvents used were obtained from E. Merck, India. The ligands used in this work were 1-alkyl-2-(naphthyl-α-azo)imidazole (α-NaiR, R = CH_3, CH_2–CH_3, CH_2–Ph) (Scheme 1) and were prepared by reported procedure [34]. Chemicals used for syntheses were of analytical grade and solvents were dried before use [35]. The solution spectral studies were carried out by spectroscopic grade solvents obtained from Lancester.

2.2. Physical measurements

Microanalyses (C, H, N) were performed using Perkin–Elmer 2400 CHN elemental analyser. Spectroscopic measurements were carried out using the following instruments: UV–Vis spectra, Lambda 25 Perkin Elmer; IR spectra (KBr disk), RX-1 Perkin Elmer; ^{1}H NMR spectra in DMSO-d_6, Bruker 300 MHz FT-NMR spectrometers in presence of TMS as internal standard. FAB-MS data were collected from Jeol-AX 500 instrument.

2.3. Preparation of compounds

2.3.1. Synthesis of [Rh(α-NaiMe-*N*,*N*′)(PPh_3)Cl_3] (**2a**)

$RhCl_3 \cdot 3H_2O$ (0.10 g, 0.379 mmol) was added to a methanol solution of α-NaiMe (0.089 g, 0.379 mmol) and PPh_3 (0.102 g, 0.379 mmol). The mixture was refluxed for 5 h under stirring condition. The red colour solution was cooled slowly in air and the products so obtained were collected by filtration, washed with cold methanol and ether and dried under vacuum. The yield was 0.16 g (58%).

All other complexes were prepared following the identical procedure. The yield varied from 55 to 65%.

*2.3.1.1. [Rh(α-NaiMe-N,N′)(PPh_3)Cl_3] (**2a**).* Microanalytical data: Found: C, 54.24; H, 3.78; N, 7.87%. Calc. for $C_{32}H_{27}N_4Cl_3PRh$: C, 54.27; H, 3.82; N, 7.91%. MS(FAB): *m/z* 709 $(M + H)^+$. FT-IR (KBr disc, cm^{-1}): ν(N=N), 1367(m); ν(C=N),1560(s); ν(Rh-Cl), 322, 330, 337; ν(PPh_3), 524, 692, 749. (w = weak; s = strong; vs = very strong; m = medium). Electronic spectral data in acetonitrile solution: (λ_{max}, nm (ε, 10^3 M^{-1} cm^{-1})): 278(17.45), 336(7.59), 374(7.32), 474 (5.897). ^{1}H NMR ($CDCl_3$): 4.11 (s, –N–CH_3, 3H), 6.86 (d, 1H J = 8.0 Hz), 7.10 (d, 1H, J = 8.0 Hz), 7.18(m, 1H), 7.05–7.55 (PPh_3), 7.60 (m, 2H), 7.81 (d, 1H, J = 8.0 Hz), 7.98 (m, 1H), 8.12 (m, 1H), 8.92 (d, 1H, J = 8.0 Hz).

*2.3.1.2. [Rh(α-NaiEt-N,N′)(PPh_3)Cl_3] (**2b**).* Microanalytical data: Found: C, 54.84; H, 4.06; N, 7.81%. Calc. for $C_{33}H_{29}N_4Cl_3PRh$: C, 54.88; H, 4.02; N, 7.76%. MS(FAB): *m/z* 723 $(M+H)^+$. FT-IR (KBr disc, cm^{-1}): ν(N=N), 1365(m); ν(C=N), 1552(s); ν(Rh-Cl), 321, 329, 338; ν(PPh_3), 527, 694, 750. (w = weak; s = strong; vs = very strong; m = medium). Electronic spectral data in acetonitrile solution: (λ_{max}, nm (ε, 10^3 M^{-1} cm^{-1})): 279(19.39), 337 (7.82), 374(6.94), 475 (5.553). ^{1}H NMR ($CDCl_3$): 1.49 (t, (–N–CH_2–)CH_3, 3H, J = 8.0 Hz), 4.48 (q, Hz, –N–CH_2, 2H, J = 7.5 Hz), 6.97 (d, 1H, J = 8.0 Hz), 7.16 (d, 1H, J = 8.0 Hz), 7.17 (m, 1H), 7.05–7.60 (PPh_3), 7.61 (m, 2H), 7.81 (d, 1H, J = 8.0 Hz), 7.96 (m, 1H), 8.14 (m, 1H), 8.90 (d, 1H, J = 8.0 Hz).

*2.3.1.3. [Rh(α-NaiCH$_2$Ph-N,N′)(PPh_3)Cl_3] (**2c**).* Microanalytical data: Found: C, 58.22; H, 3.90; N, 7.11%. Calc. for $C_{38}H_{31}N_4Cl_3PRh$: C, 58.20; H, 3.96; N, 7.15%. MS(FAB): *m/z* 785 $(M + H)^+$. FT-IR (KBr disc, cm^{-1}): ν(N=N), 1366(m); ν(C=N), 1563(s); ν(Rh-Cl), 320, 327, 337;

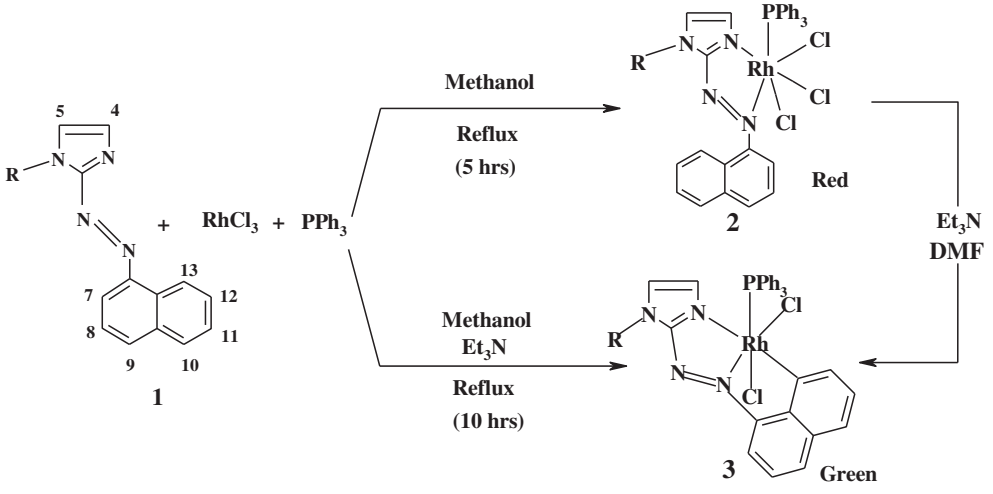

α-NaiR (**1**); R = -CH_3 (**1a, 2a, 3a**), -CH_2CH_3 (**1b, 2b, 3b**), -CH_2Ph (**1c, 2c, 3c**)

Scheme 1. The ligands (α-NaiR, **1**) and the complexes, [Rh(α-NaiR-*N*,*N*′)(PPh_3)Cl_3] (**2**) [Rh(α-NaiR-*N*,*N*′C)(PPh_3)Cl_2] (**3**).

ν(PPh_3), 526, 692, 749. (w = weak; s = strong; vs = very strong; m = medium). Electronic spectral data in acetonitrile solution: (λ_{max}, nm (ε, 10^3 M^{-1} cm^{-1})): 278(16.57), 337 (6.92), 373(6.21), 475 (5.234). ^{1}H NMR ($CDCl_3$): 5.54 (s, −N−CH_2, 2H), 7.09 (d, 1H, J = 8.0 Hz), 7.22 (d, 1H, J = 8.0 Hz), 7.20 (m, 1H), 7.05−7.55 (PPh_3), 7.25−7.35 (−N−(CH_2)Ph, 5H), 7.60 (m, 2H), 7.84 (d, J = 8.0 Hz, 1H), 7.99 (m, 1H), 8.11 (m, 1H), 8.85 (d, 1H, J = 8.0 Hz).

2.3.2. Synthesis of [Rh(α-NaiMe-N,N′,C)(PPh_3)Cl_2] (**3a**)

(a) Direct synthesis

1-Methyl-2-(naphthyl-α-azo)imidazole (α-NaiMe) (0.089 g, 0.379 mmol) was dissolved in 50 ml methanol and Et_3N (0.038 g, 0.376 mmol) was added. The solution was stirred for 5 min. Then $RhCl_3 \cdot 3H_2O$ (0.1 g, 0.379 mmol) and PPh_3 (0.102 g, 0.379 mmol) were added and the mixture was refluxed for 12 h under stirring condition to yield a deep green solution. Evaporation of this solution gave a dark green solid, which was subjected to purification by silica gel column chromatography prepared in petroleum−ether (60−80 °C fraction). A green portion was eluted with 1:1(v/v) benzene−acetonitrile which upon evaporation afforded analytically pure product **3a**. Yield was 0.17 g (67%).

All other complexes were prepared by the same procedure. The yield varied from 60 to 65%.

*2.3.2.1. [Rh(α-NaiMe-N,N′,C)(PPh_3)Cl_2] (**3a**).* Microanalytical data: Found: C, 57.18; H, 3.90; N, 8.36%. Calc. for $C_{32}H_{26}N_4Cl_2PRh$: C, 57.22; H, 3.87; N, 8.35. MS(FAB): m/z 672 $(M + H)^+$. FT-IR (KBr disc, cm^{-1}): ν(N=N), 1381(m); ν(C=N), 1576(s); ν(Rh-Cl), 321, 327; ν(PPh_3), 524, 695, 749. (w = weak; s = strong; vs = very strong; m = medium). Electronic spectral data in acetonitrile solution: (λ_{max}, nm (ε, 10^3 M^{-1} cm^{-1})): 277 (37.22), 384 (29.17), 429 (21.00), 622 (11.45). ^{1}H NMR ($CDCl_3$): 4.06 (s, −N−CH_3, 3H), 7.09 (d, 1H, J = 8.0 Hz), 7.17(d, 1H, J = 8.0 Hz), 7.26−7.45 (PPh_3), 7.46 (m, 2H), 7.59 (m, 1H), 7.71 (m, 1H), 7.91 (m, 1H), 8.08 (d, 1H, J = 8.0 Hz).

*2.3.2.2. [Rh(α-NaiEt-N,N′,C)(PPh_3)Cl_2] (**3b**).* Microanalytical data: Found: C, 57.80; H, 4.10; N, 8.15%. Calc. for $C_{33}H_{28}Cl_2N_4PRh$: C, 57.81; H, 4.09; N, 8.18%. MS(FAB): m/z 686 $(M + H)^+$. FT-IR (KBr disc, cm^{-1}): ν(N=N),1371(m); ν(C=N), 1573(s); ν(Rh-Cl), 321, 328; ν(PPh_3), 521, 697, 762. (w = weak; s = strong; vs = very strong; m = medium). Electronic spectral data in acetonitrile solution: (λ_{max}, nm (ε, 10^3 M^{-1} cm^{-1})): 277 (37.22), 385(29.16), 430(15.65), 622(7.84). ^{1}H NMR ($CDCl_3$): 1.41 (t, (−N−CH_2−)CH_3, 3H, J = 8.0 Hz), 4.27 (q, −N−CH_2, 2H, J = 7.5 Hz), 7.11 (d, 1H, J = 8.0 Hz), 7.16(d, 1H, J = 8.0 Hz), 7.26−7.42 (PPh_3), 7.43 (m, 2H), 7.58 (m, 1H), 7.71 (m, 1H), 7.89 (m, 1H), 8.06 (d, 1H, J = 8.0 Hz).

*2.3.2.3. [Rh(α-NaiCH_2Ph-N,N′,C)(PPh_3)Cl_2] (**3c**).* Microanalytical data: Found: C, 61.06; H, 4.03; N, 7.47%. Calc. for $C_{38}H_{30}Cl_2N_4PRh$: C, 61.04; H, 4.02; N, 7.49%. MS(FAB): m/z 748 $(M + H)^+$. FT-IR (KBr disc, cm^{-1}): ν(N=N), 1372(m); ν(C=N), 1575 (s); ν(Rh-Cl), 321, 330; ν(PPh_3), 525, 698, 750. (w = weak; s = strong; vs = very strong; m = medium). Electronic spectral data in acetonitrile solution: (λ_{max}, nm (ε, 10^3 M^{-1} cm^{-1})): 277 (32.09), 384 (17.02), 429 (15.90), 622 (8.23). ^{1}H NMR ($CDCl_3$): 5.52 (q, −N−CH_2, 2H, J = 7.8 Hz), 7.16 (d, 1H, J = 8.0 Hz), 7.28(d, 1H, J = 8.0 Hz), 7.20−7.45 (PPh_3), 7.44 (m, 2H), 7.56 (m, 1H), 7.73 (m, 1H), 7.92 (m, 1H), 8.09 (d, 1H, J = 8.0 Hz).

(b) Conversion of coordination to cyclometallated Rh(III) complexes

*[Rh(α-NaiMe-N,N′)(PPh_3)Cl_3] (**2a**) → [Rh(α-NaiMe-N,N′,C)(PPh_3)Cl_2] (**3a**)*

*2.3.2.4. [Rh(α-NaiMe-N,N′)(PPh_3)Cl_3] (**2a**).* (0.1 mg, 0.141 mmol) was dissolved in 50 ml DMF and Et_3N (0.014 g, 0.141 mmol) was added. Then it was refluxed for 7 h under stirring condition in inert atmosphere (N_2) to yield a deep green solution. Slow evaporation of this solution gave a dark green solid, which was subjected to purification by silica gel column chromatography prepared in petroleum−ether (60−80 °C fraction). A green portion was eluted with 1:1(v/v) benzene−acetonitrile mixture which upon evaporation afforded analytically pure product **3a**. Yield was 0.055 g (59%).

2.4. X-ray diffraction study

Details of crystal analyses, data collection and structure refinement data are given in Table 1. Single crystal data were collected by fine focus sealed tube using fine focus graphite monochromator Bruker Smart CCD Area Detector (Mo-Kα radiation, (λ = 0.71073 Å) for [Rh(α-NaiEt-*N*, *N*′)(PPh_3)Cl_3] (**2b**) (crystal size, 0.44 × 0.08 × 0.06 mm) at 293(2) K and for [Rh(α-NaiEt-*N*, *N*′,C)(PPh_3)Cl_2] (**3b**) (crystal size, 0.50 × 0.16 × 0.04 mm) at 298(2) K. Unit cell parameters were determined from least-squares refinement of setting angles with θ in the range $2.49 \le \theta \le 26.01°$ (**2b**) and $1.67 \le \theta \le 25.00°$ (**3b**). Out of 16,493 collected data 5906 for **2b** and 28,001 collected data 5177 for **3b** with $I > 2\sigma(I)$ were used for structure solution. The hkl range are $-12 \le h \le 14$; $-19 \le k \le 17$; $-21 \le l \le 21$ for **2b**, $-10 \le h \le 10$; $-26 \le k \le 26$; $-17 \le l \le 17$ for **3b**. Reflection data were recorded using the ω scan technique. Data were corrected for Lorentz polarization effects and for linear decay. The structure was solved by direct method for all these compounds using SHELXS-97 [36] and successive difference Fourier syntheses. Largest difference in peak and hole (e.Å^{-3}) are −0.323, 0.806 (**2b**) and −0.239, 0.466 (**3b**). All non-hydrogen atoms were refined anisotropically. The hydrogen atoms were fixed geometrically and refined using the riding model. All calculations were carried out using SHELXL-97 [37], ORTEP-32 [38], and PLATON-99 [39] programs.

2.5. Computational details

All computations were performed using the Gaussian03 (G03) software package running under Windows [40]. The Becke's three-

Table 1
Selected crystallographic data for **2b** and **3b**.

	[Rh(α-NaiEt-*N*,*N*′)(PPh_3)Cl_3] (**2b**)	[Rh(α-NaiEt-*N*,*N*′,C)(PPh_3)Cl_2] (**3b**)
Empirical formula	$C_{33}H_{29}N_4PCl_3Rh \cdot H_2O$	$C_{33}H_{28}N_4PC_{l2}$ Rh
Formula weight	739.85	685.37
T, K	298(2)	298 (2)
Crystal system	Orthorhombic	Monoclinic
Space group	*Pna*2(1)	*P*2(1)/*n*
a, Å	11.5353(8)	9.1216(8)
b, Å	15.4737(11)	21.8811(19)
c, Å	17.4878(12)	14.7889(13)
β, °	90.00	94.437(2)
V, Å^3	3121.5(4)	2942.9(4)
Z	4	4
D_{calc} (mg m^{-3})	1.574	1.547
λ (Å)	0.71073	0.71073
μ (Mo-Kα) (mm^{-1})	0.885	0.847
Total reflection	17,036	28,001
Unique reflections [$I > 2\sigma(I)$]	6055	5177
Refined parameters	389	371
Goodness-of-fit on F^2	0.999	1.062
θ range (°)	1.76−26.01	1.67−25.00
R (F_o)[a] [$I > 2\sigma(I)$]	0.0465	0.0312
wR (F_o)[b] [$I > 2\sigma(I)$]	0.0961	0.0764

[a] $R = \Sigma||F_o| - |F_c||/\Sigma|F_o|$.
[b] $wR = [\Sigma w(F_o^2 - F_c^2)^2/\Sigma w(F_o^2)^2]^{1/2}$, $w = 1/[\sigma^2(F_o)^2 + (0.0433P)^2 + 0.0000P]$ (**2b**) and $w = 1/[\sigma^2(F_o)^2 + (0.0377P)^2 + 1.4388P]$ (**3b**) where $P = ((F_o^2 + 2F_c^2)/3$.

parameter hybrid exchange functional and the Lee–Yang–Parr nonlocal correlation functional (B3LYP) was used throughout this computation [41]. For heavy atoms like rhodium, phosphorus and chlorine the Los Alamos effective core potential plus double zeta (LanL2DZ) basis set were employed [42] while other elements were assigned by 6-31G basis set. The geometric structures of the ligand and the complexes in the ground state (S_0) were fully optimized at the B3LYP level. Geometry optimization was carried out from the geometry obtained from the crystal structure without any symmetry constraints. In all cases, vibrational frequencies were calculated to ensure that optimized geometries represented local minima. Using the respective optimized S_0 geometries we employed time dependent density functional theory (TD-DFT) at the B3LYP level to predict their absorptions characteristics [43]. Although CAM-B3LYP could improve excitation energies and the assignment would be more appropriate but the configuration of computation workstation has not been sustained. We have been failed to carry out calculation using CAM-B3LYP functional.

3. Results and discussion

3.1. Synthesis

1-Alkyl-2-(naphthyl-α-azo)imidazole (Scheme 1: α-NaiR, **1**; R = CH_3 (**a**), CH_2-CH_3 (**b**), CH_2Ph (**c**)) generally serve as *N*, *N*′chelating ligand where, *N*(imidazolyl) and *N*(azo) are assigned to *N* and *N*′ respectively. The reaction of $RhCl_3$ with α-NaiR (**1**) and PPh_3 in methanol under refluxing condition has synthesized a red colour complex, **2**. The X-ray structure of one of the complexes, **2b** reveals that α-NaiEt binds to Rh(III) centre as *N*, *N*′ chelating agent. On the other hand, upon addition of Et_3N to the same reaction mixture has synthesized a green colour rhodium(III) complex, **3**, where the ligand has been found to undergo C–H activation. The C–H activation at the 13th-position (C(13)–H) of the naphthyl ring has been confirmed by the X-ray crystal structure of complex **3b**, where the ligand α-NaiR coordinates with rhodium as monoanionic tridentate *N*, *N*′, C chelating agent. The cyclomtallated complexes, **3**, can be synthesised by refluxing **2** in basic medium (Et_3N) (shown in Scheme 1). The formulation of the complexes is also consistent with the microanalytical and spectroscopic data. All the complexes are diamagnetic, indicating the presence of rhodium in the +3 oxidation state (d^6).

3.2. Molecular structure of [Rh(α-NaiEt-N, N′)(PPh_3)Cl_3] (**2b**) and [Rh(α-NaiEt-N, N′,C)(PPh_3)Cl_2] (**3b**)

The complexes **2b** and **3b** were crystallized by slow diffusion of hexane into dichloromethane solution of the respective complexes. Suitable crystals were picked up for X-ray analyses. The structures are shown in Figs. 1 and 2 and the relevant bond parameters are given in Table 2. The ligand is coordinated to Rh(III) as a bidentate (*N*, *N*′) donor in **2b** and makes a five-member chelate ring with a bite angle ∠N(4)–Rh(1)–N(1), 77.47(19)° (Table 2) and as a monoanionic tridentate (*N*, *N*′, C) donor, forming two adjacent five-member chelate rings with bite angles ∠N(3)–Rh(1)–N(1), 74.86(9)° and ∠N(1)–Rh(1)–C(30), 82.92(10)° (Table 2) in **3b**. α-NaiEt acts as a *N*, *N*′ chelator in **2b** and the coordination geometry for the central Rh atom is based on an octahedron defined by a N_2PCl_3 coordination set. The Rh-Cl distances are comparable with reported Rh(III)-1-alkyl-2-(arylazo)imidazole complexes [44]. However, the N(azo)–Rh–N(imidazolyl) chelate angles are shorter than **2b** which may be due to the structural strain originated from bulkier naphthyl pendant group and coordinated PPh_3 [44]. In **3b**, α-NaiEt acts as a tridentate chelator where one of the donor centres is naphthyl carbanion, (C(30)) along with *N* and *N*′ donor centres.

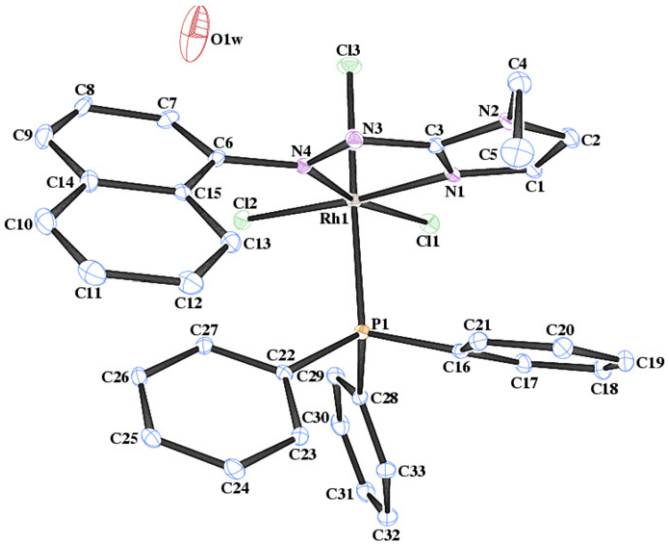

Fig. 1. Single crystal X-ray structure of [Rh(α-NaiR-*N*, *N*′)(PPh_3)Cl_3] (**2b**).

The Rh–N(imidazolyl), (N(3)) (2.271(2) Å) of **3b**, *trans* to Rh–C, is longer than Rh–N(imidazolyl), (N(1)) (2.000(4) Å) of **2b** which may be due to the stronger *trans* effect of aryl carbon (Rh–C) and the angular strain developed in the ligand frame due to double chelation. The Rh–P bond distances (Rh(1)–P(1), 2.3133(4) Å in **2b** and Rh(1)–P(1), 2.2995(7) Å in **3b**) are comparable with the published results [45].

These two structures are optimized using DFT computation technique. The experimental bond distances are lower than calculated lengths in general by 0.02–0.15 Å while the bond angles are elongated by 1–2° (Table 2). This implies compatibility of methods used for calculation and hence the derived functions are closer to the experiments.

The packing of molecular structure **2b** shows the presence of crystallized H_2O molecule which is hydrogen bonded with one of the Cl of three Rh–Cl groups (Fig. 3) (O(1)–H(2)–Cl(3): H(2)–Cl(3), 2.69 (2) Å; O(1)––Cl(3), 3.448(8) Å and ∠O(1)–H(2)–Cl(3), 149.0 °). Each unit is then connected by C–H–π interaction, C(20)–H(20)–Cg(1) (H(20)–Cg(1), 2.91 Å; C(20)–Cg(1), 3.485(6) Å and ∠C(20)–H(20)–Cg(1), 121° at symmetry −1/2 + *x*, 3/2 − *y*, *z*

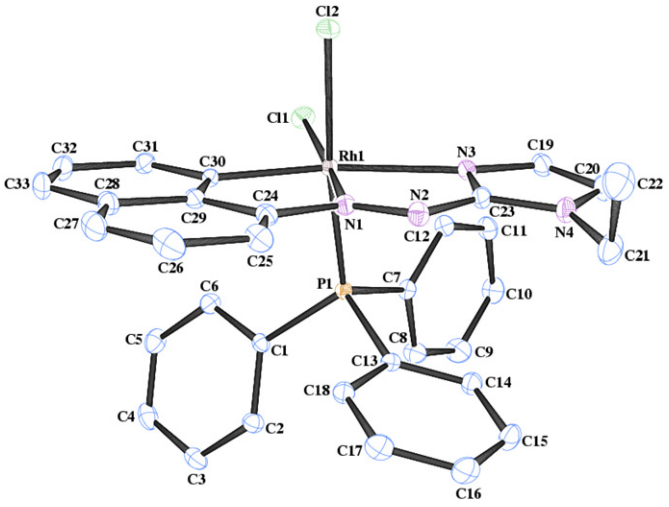

Fig. 2. Single crystal X-ray structure of [Rh(α-NaiEt-*N*, *N*′, C)(PPh_3)Cl_2] **(3b)**.

Table 2
Selected experimental and theoretical bond lengths (Å) and angles (°) for the complexes [Rh(α-NaiEt-*N*, *N*′)(PPh_3)Cl_3] **(2b)** and [Rh(α-NaiEt-*N*, *N*′, C)(PPh_3)Cl_2] **(3b)**.

Bond length (Å)	Experimental value	Theoretical value	Bond angle (°)	Experimental value	Theoretical value
[Rh(α-NaiEt-N,N′)(PPh_3)Cl_3] ***(2b)***					
Rh(1)–N(1)	2.000(4)	2.023	N(4)–Rh(1)–N(1)	77.43(18)	77.70
Rh(1)–N(4)	2.084(5)	2.138	N(4)–Rh(1)–Cl(2)	100.44(13)	99.33
Rh(1)–P(1)	2.313(13)	2.475	N(4)–Rh(1)–Cl(3)	84.77(13)	84.64
Rh(1)–Cl(1)	2.330(14)	2.425	N(4)–Rh(1)–P(1)	95.61(13)	98.17
Rh(1)–Cl (2)	2.344(12)	2.443	N(1)–Rh(1)–Cl(1)	89.50(15)	89.59
Rh(1)–Cl (3)	2.425(14)	2.457	N(1)–Rh(1)–Cl(3)	85.61(11)	86.29
N(3)–N(4)	1.270(6)	1.314	N(1)–Rh(1)–P(1)	92.76(11)	93.89
N(1)–C(3)	1.332(7)	1.354	Cl(2)–Rh(1)–Cl(1)	92.40(6)	93.34
N(3)–C(3)	1.367(6)	1.372	Cl(2)–Rh(1)–Cl(3)	91.38(6)	92.83
P(1)–C(16)	1.811(5)	1.880	Cl(2)–Rh(1)–P(1)	91.24(5)	87.14
P(1)–C(22)	1.833(5)	1.889	Cl(1)–Rh(1)–P(1)	87.86(6)	85.37
P(1)–C(28)	1.836(5)	1.889	Cl(1)–Rh(1)–Cl(3)	91.38(6)	91.80
			N(4)–Rh(1)–Cl(1)	166.60(12)	166.98
			N(1)–Rh(1)–Cl(2)	175.64(13)	176.97
			P(1)–Rh(1)–Cl(3)	178.20(6)	177.16
[Rh(α-NaiEt-N,N′)(PPh_3)Cl_2] ***(3b)***					
Rh(1)–N(1)	1.982(2)	2.006	N(1)–Rh(1)–N(3)	74.86(9)	76.41
Rh(1)–N(3)	2.271(2)	2.253	N(1)–Rh(1)–C(30)	82.92(10)	82.73
Rh(1)–P(1)	2.2995(7)	2.464	N(1)–Rh(1)–Cl(2)	84.78(6)	84.82
Rh(1)–C(30)	2.003(3)	2.018	N(1)–Rh(1)–P(1)	95.53(6)	95.40
Rh(1)–Cl(1)	2.3577(8)	2.448	N(3)–Rh(1)–Cl(1)	109.57(6)	102.90
Rh(1)–Cl(2)	2.3897(7)	2.448	N(3)–Rh(1)–Cl(2)	88.50(6)	86.84
N(1)–N(2)	1.269(3)	1.305	N(3)–Rh(1)–P(1)	86.24(6)	91.68
N(2)–C(23)	1.370(4)	1.382	C(30)–Rh(1)–Cl(1)	92.51(8)	97.63
N(3)–C(23)	1.347(4)	1.360	C(30)–Rh(1)–Cl(2)	88.89(7)	88.57
P(1)–C(1)	1.826(3)	1.888	C(30)–Rh(1)–P(1)	96.64(8)	92.89
P(1)–C(7)	1.834(3)	1.890	P(1)–Rh(1)–Cl(1)	89.99(3)	89.13
P(1)–C(13)	1.822(3)	1.882	Cl(1)–Rh(1)–Cl(2)	90.11(3)	90.62
			N(1)–Rh(1)–Cl(1)	173.19(7)	175.54
			N(3)–Rh(1)–C(30)	157.77(10)	158.93
			P(1)–Rh(1)–Cl(2)	174.46(3)	178.38

where Cg(1) refers to C(22)–C(23)–C(24)–C(25)–C(26)–C(27) and is leading to the formation of 1D supramolecular chain along crystallographic *a*-axis (Fig. 4).

3.3. Spectroscopic characterization

The IR spectra of the complexes display a moderately strong band in the region 1365–1380 cm^{-1} for ν(N═N) stretching vibrations and a weak band in the region 1560–1575 cm^{-1} for ν(C═N) stretching vibrations which are significantly shifted to lower value

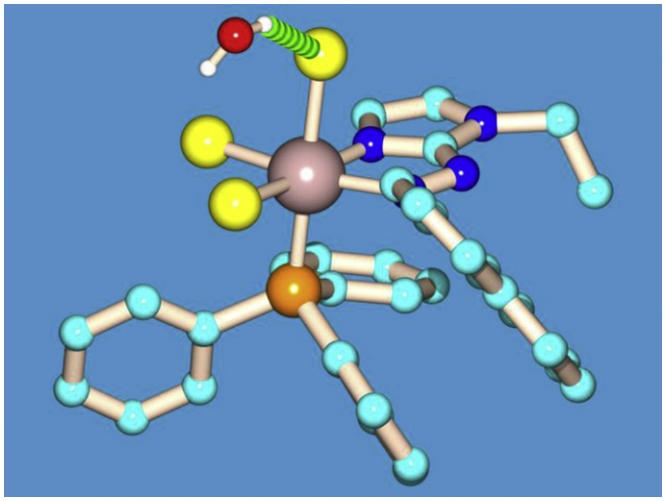

Fig. 3. Water molecule is bounded to the moiety through hydrogen bonding interactions in **2b**.

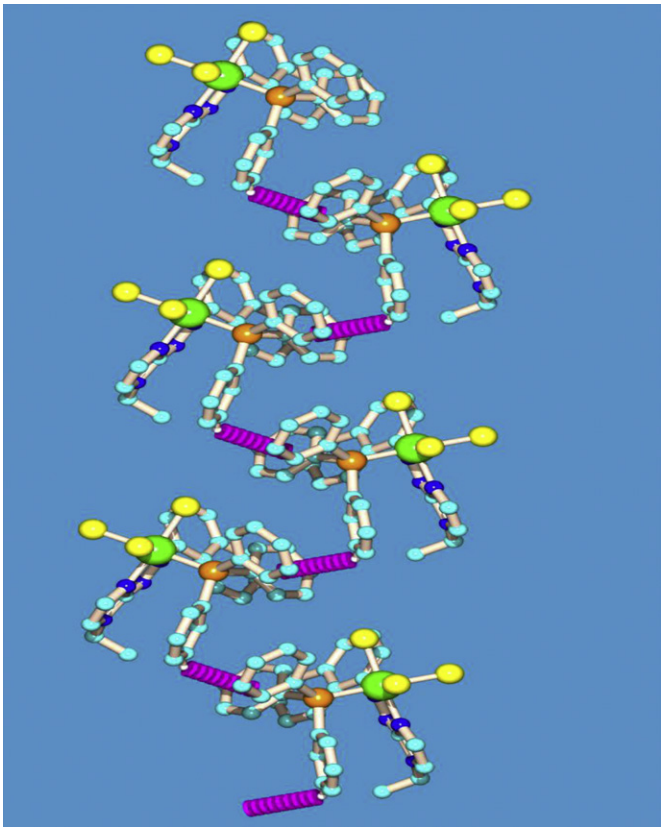

Fig. 4. 1D supramolecular chain is formed by C–H–π interactions along crystallographic ***a***-axis in **2b**.

compared to free ligand by 25–30 cm^{-1}. This supports the coordination of ligand (α-NaiR) to Rh(III) through N(azo) and N(imidazolyl). The spectra also show three characteristics strong bands around 750, 695 and 525 cm^{-1} for coordinated PPh_3 ligand.

The electronic spectra of the complexes were recorded in acetonitrile solution. The colour of the solution of **2** is red and that of **3** is green. Both the complexes (**2**, **3**) show four major peaks of high intensity (ε, 10^4 M^{-1} cm^{-1}) in 250–650 nm (Fig. 5). The transitions at ultraviolet region may be assigned as intraligand transitions and that of visible regions are probably due to metal-to-ligand charge transfer transitions. Multiple charge-transfer transitions in such mixed-ligand complexes may result from lower symmetry splitting of the metal level, the presence of different acceptor orbitals, and the mixing of singlet and triplet configurations in the excited state through spin-orbit coupling [46–48]. The spectral assignment have been done by theoretical computation of optimized geometries using DFT and TD-DFT technique (*vide infra*). The spectra of **3** differ from **2** in the longer wavelength region (>600). The cyclometallated compound (**3**) has characteristic low energy band and may be due to the lowering of symmetry of double chelation that restricts vibrational relaxation.

The ^{1}H-NMR spectra of the complexes are studied in DMSO-d_6 and assignment has been made on comparing with free ligand data [33,34] and intensity measurement of the signals corresponds to the total number of protons in the respective complexes. In the coordination complexes, **2**, the protons suffer significant downfield shifting compared to the ligands values, which may be due to the electron-withdrawing effect of the coordinated rhodium(III). The imidazole protons, 4-H and 5-H experience ~0.05–0.20 ppm downfield shift compared to free ligand values and appeared as singlets. In the cyclometallated complexes, **3**, the imidazole protons shift to upperfield region compared to the coordination complexes (**2**). This indicates that the cyclometallated complexes (**3**) have more contribution of metal d-orbital in the formation of molecular orbital compare to coordination complexes. The DFT calculation also supports the contribution of orbitals of Rh to HOMO (Supplementary materials, Table S1). The resonances of the phenyl protons of PPh_3 were observed as multiplets at 7.00–7.60 ppm.

3.4. DFT and TD-DFT calculation

The DFT computations of [Rh(α-NaiEt-*N*, *N*′)(PPh_3)Cl_3] (**2b**) and [Rh(α-NaiEt-*N*, *N*′,C)(PPh_3)Cl_2] (**3b**) have been performed with optimized geometry to correlate the electronic structure with the

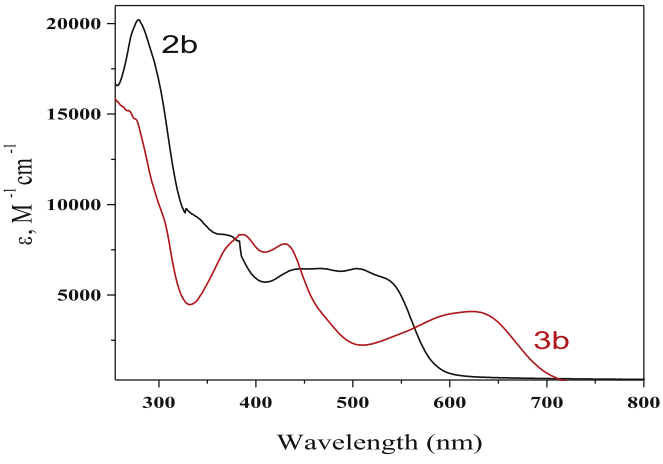

Fig. 5. UV–visible spectra of [Rh(α-NaiEt-*N*, *N*′)(PPh_3)Cl_3] (**2b**) and [Rh(α-NaiEt-*N*, *N*′, C)(PPh_3)Cl_2] (**3b**) in acetonitrile.

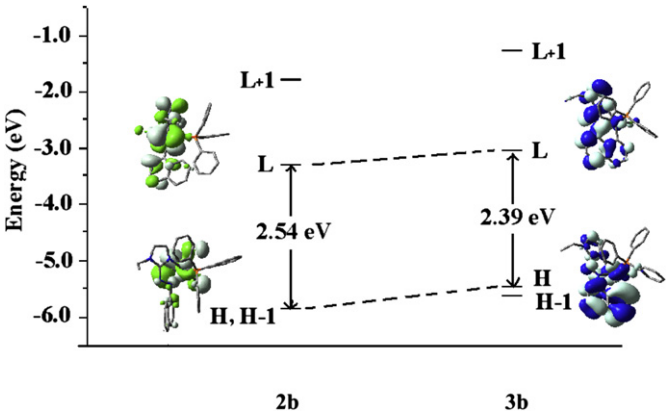

Fig. 6. Correlation diagram between [Rh(α-NaiEt-*N*, *N*′)(PPh_3)Cl_3] (**2b**) and [Rh(α-NaiEt-*N*, *N*′, C)(PPh_3 Cl_2)] (**3b**).

observed electronic spectra. The electronic structure and configuration are dependent on the composition and stereochemistry in the molecule. The HOMO of **3b** lies at higher energy by 0.4 eV than that of **2b** (**3b**, E_{HOMO} = −5.44 eV; **2b**, E_{HOMO} = −5.84 eV). The LUMO also follows same trend and the energy difference is 0.25 eV (**3b**, E_{LUMO} = −3.05 eV; **2b**, E_{LUMO} = −3.30 eV) (Fig. 6). Other occupied MOs are closely spaced in **2b** (HOMO-1, −5.87 eV; HOMO-2, −5.97 eV) and **3b** (HOMO-1, −5.61 eV; HOMO-2, −5.64 eV) but a substantial energy gap is observed between LUMO and LUMO + 1 ($\Delta E > 0.3$ eV) (Table S1, Supplementary materials). In **2b**, the HOMO is dominated by Cl (84%) function with a small contribution from rhodium (9%); whereas in **3b**, it is composed of α-NaiEt (61%), Cl (18%) and Rh (19%). Other occupied MOs (HOMO-1 to HOMO-5) for **2b** have the major contribution from Cl function (65–85%) with contribution from rhodium as well (4–25%). The similar observation is recorded in **3b**. The LUMO is dominated by ligand function (92%) in these complexes; in addition to that in **3b**, the unoccupied MOs like LUMO + 1 to LUMO + 4 have contribution from PPh_3 (55–85%).

To gain an insight about the nature of electronic transitions and to explain the electronic spectra, the TD-DFT calculations were performed. The experimental spectra correlate well with the theoretical spectra (Supplementary materials, Fig. S1). The calculations also interpret multiple charge transfer transitions for these complexes. For complex **2b**, the experimental spectrum shows transition at 475 nm which has been correlated with admixture of HOMO → LUMO and HOMO-n → LUMO in the calculated spectrum (501 nm) (Supplementary materials, Table S2). The bands in the experimental spectrum of **2b** at 275–380 nm are assigned to the mixture of multiple transitions originated from ILCT, XLCT, XMCT (pπ (Cl) → dπ (Rh)) etc. For complex **3b**, the lowest energy transition near 622 nm is originated from HOMO → LUMO. The other transition near 430 nm region is due to transition from HOMO-2/HOMO-3 → LUMO and can be assigned as chloride-to-ligand and intraligand charge transfer transitions. The transitions at shorter wavelengths are mixture of mainly PPh_3-to-ligand (YLCT), intraligand (ILCT), chloride-to-ligand charge transfer transitions (XLCT).

4. Conclusion

The coordination and cyclometallated complexes of Rh(III) incorporating 1-alkyl-2-(naphthyl-α-azo)imidazole (α-NaiR) are described in this paper. Organorhodium complexes are obtained on treatment of α-NaiR with $RhCl_3$ in presence of Et_3N. The coordination complexes also transfer to the organometallic complexes with the treatment of Et_3N. The complexes are characterized by IR,

UV–VIS, ^{1}H-NMR spectral data and the structures of both types of complexes are confirmed by single crystal X-ray diffraction study. The electronic properties are explained by DFT and TD-DFT calculations. We will study the C–H activation reaction by other platinum group metals and the reactivity of the M–C bonds.

Acknowledgements

Financial support from Council of Scientific and Industrial Research, and Department of Science and Technology, New Delhi are gratefully acknowledged.

Appendix A. Supplementary material

Energy and composition of the selected frontier molecular orbitals calculated by DFT and electronic transition data from TDDFT calculation are given in Supplementary material. Crystallographic data for the structural analysis are in the Cambridge Crystallographic Data Centre, and CCDC No. 907997, [Rh(α-NaiEt-*N*, *N*′)(PPh_3)Cl_3] (**2b**) and 907996 [Rh(α-NaiEt-*N*, *N*′,C)(PPh_3)Cl_2] (**3b**). Copies of this information may be obtained free of charge from the Director, CCDC, 12 Union Road, Cambridge, CB2 1FZ, UK (email: deposit@ccdc.cam.ac.uk or http://www.ccdc.cam.ac.uk).

References

[1] K. Venkataraman, The Chemistry of Synthetic Dyes, Academic Press, New York, 1956.
[2] H. Zollinger, Color Chemistry: Syntheses, Properties and Application of Organic Dyes and Pigments, second ed., VCH, Weinheim, 1991.
[3] S. Kawata, Y. Kawata, Chem. Rev. 100 (2000) 1777–1788.
[4] J.A. Delaire, K. Nakatani, Chem. Rev. 100 (2000) 1817–1845.
[5] I. Sener, F. Karc, N. Ertan, E. Kılıc, Dyes Pigments 70 (2006) 143–148.
[6] W. Huang, Dyes Pigments 79 (2008) 69–75.
[7] G. Pavlovic, L. Racane, H. Cicak, V. Tralic-Kulenovic, Dyes Pigments 83 (2009) 354–362.
[8] F. Hamon, F. Djedaini-Pilard, F. Barbot, C. Len, Tetrahedron 65 (2009) 10105–10123.
[9] B.K. Ghosh, A. Chakravorty, Coord. Chem. Rev. 95 (1989) 239–266.
[10] N. Bag, A. Pramanik, G.K. Lahiri, A. Chakravorty, Inorg. Chem. 31 (1992) 40–45.
[11] A.C.G. Hotze, H. Kooijman, A.L. Spek, J.G. Haasnoot, J. Reedijk, New J. Chem. 28 (2004) 565–569.
[12] C. Das, A. Saha, C.-H. Hung, G.-H. Lee, S.-M. Peng, S. Goswami, Inorg. Chem. 42 (2003) 198–204.
[13] K.N. Mitra, S. Goswami, Proc. Indian Acad. Sci. (Chem. Sci) 111 (1999) 461–467.
[14] B.K. Santra, G.K. Lahiri, J. Chem. Soc. Dalton Trans. (1998) 1613–1618.
[15] G.K. Lahiri, S. Bhattacharya, S. Goswami, A. Chakravorty, J. Chem. Soc. Dalton Trans. (1990) 561–565.
[16] T.K. Misra, D. Das, C. Sinha, P. Ghosh, C.K. Pal, Inorg. Chem. 37 (1998) 1672–1678.
[17] P. Byabartta, Sk. Jasimuddin, B.K. Ghosh, C. Sinha, A.M.Z. Slawin, J.D. Woollins, New J. Chem. 26 (2002) 1415–1424.
[18] P. Byabartta, J. Dhinda, P.K. Santra, C. Sinha, K. Panneerselvam, F.-L. Liao, T.-H. Lu, J. Chem. Soc. Dalton Trans. (2001) 2825–2832.
[19] J. Otsuki, K. Suwa, K. Narutaki, C. Sinha, I. Yoshikawa, K. Araki, J. Phys. Chem. A 109 (2005) 8064–8069.
[20] K.K. Sarker, B.G. Chand, K. Suwa, J. Cheng, T.-H. Lu, J. Otsuki, C. Sinha, Inorg. Chem. 46 (2007) 670–680.
[21] A.D. Ryabov, Synthesis (1985) 233–252.
[22] J.P. Collman, L.S. Hegedus, J.R. Norton, R.G. Finke, Principles and Applications of Organotransition Metal Chemistry. Mill Valley, CA (1987).
[23] M. Bellar, C. Bolm, Transition Metals for Organic Synthesis 1–2, Wiley-VCH, Weinheim, 1998.
[24] B. Cornils, W.A. Hermann (Eds.), Applied Homogenous Catalysis with Organometallic Compounds: A Comprehensive Handbook in Two Volumes, VCH, Weinheim, 1996.
[25] J. Tsuji, Transition Metal Reagents and Catalysts, Wiley-VCH, Weinheim, 2000.
[26] I. Aiello, A. Crispini, M. Ghedini, M. La Deda, F. Barigelletti, Inorg. Chim. Acta 308 (2000) 121–128.
[27] D.P. Lydon, G.W.V. Cave, J.P. Rourke, J. Mater. Chem. 7 (1997) 403–406.
[28] L. Dıez, P. Espinet, J.A. Miguel, M.P.R. Medina, J. Organomet. Chem. 690 (2005) 261–268.
[29] C.N. Ranninger, I.L. Solera, J. Rodriguez, J.L.G. Ruano, P.R. Raithby, J.R. Masaguer, C. Alosona, J. Med. Chem. 36 (1993) 3795–3801.
[30] W. Kaim, B. Schwederski, Bioinorganic Chemistry: Inorganic Elements in the Chemistry of Life, J. Wiley & Sons, Chichester–New York–Brisbane–Toronto Singapore, 1994.
[31] S.J. Lippard, J.M. Berg, Principles of Bioinorganic Chemistry, University Science Books, Mill Valley, CA, 1994.
[32] E. Gómez, M.A. Huertos, J. Pérez, L. Riera, A. Menéndez-Velázquez, Inorg. Chem. 49 (2010) 9527–9534.
[33] J. Dinda, D. Das, P.K. Santra, C. Sinha, L.R. Falvello, J. Organomet. Chem. 629 (2001) 28–38.
[34] J. Dinda, K. Bag, C. Sinha, G. Mostafa, T.-H. Lu, Polyhedron 22 (2003) 1367–1376.
[35] A.I. Vogel, A Text Book of Practical Organic Chemistry, Longmann, London, 1959.
[36] G.M. Sheldrick, SHELXS-97, Program for the Solution of Crystal Structure, University of Gottingen, Germany, 1997.
[37] G.M. Sheldrick, SHELXL 97, Program for the Refinement of Crystal Structure, University of Gottingen, Germany, 1997.
[38] L.J. Farrugia, J. Appl. Cryst. 30 (1997) 565.
[39] A.L. Spek, PLATON, Molecular Geometry Program, University of Utrecht, The Netherlands, 1999.
[40] M.J. Frisch, G.W. Trucks, H.B. Schlegel, P.M.W. Gill, B.G. Johnson, M.A. Robb, J.R. Cheeseman, T.A. Keith, G.A. Petersson, J.A. Montgomery, K. Raghavachari, M.A. Al-Laham, V.G. Zakrzewski, J.V. Ortiz, J.B. Foresman, J. Cioslowski, B.B. Stefanov, A. Nanayakkara, M. Challacombe, C.Y. Peng, P.Y. Ayala, W. Chen, M.W. Wong, J.L. Andres, E.S. Replogle, R. Gomperts, R.L. Martin, D.J. Fox, J.S. Binkley, D.J. Defrees, J. Baker, J.P. Stewart, M. Head-Gordon, C. Gonzalez, J.A. Pople, Gaussian98, Gaussian, Inc., Pittsburgh, PA, 1998.
[41] C. Lee, W. Yang, R.G. Parr, Phys. Rev. B 37 (1988) 785–789.
[42] P.J. Hay, W.R. Wadt, J. Chem. Phys. 82 (1985) 270–283.
[43] M. Cossi, V.J. Barone, J. Chem. Phys. 115 (2001) 4708–4717.
[44] D. Sardar, P. Datta, S. Das, B. Saha, S. Samanta, D. Bhattacharya, P. Karmakar, C.-D. Chen, C.-J. Chen, C. Sinha, Inorg. Chim. Acta 394 (2013) 98–106.
[45] R. Acharyya, S. Dutta, F. Basuli, S.-M. Peng, G.-H. Lee, L.R. Falvello, S. Bhattacharya, Inorg. Chem. 45 (2006) 1252–1259.
[46] B.J. Pankuch, D.E. Lacky, G.A. Crosby, J. Phys. Chem. 84 (1980) 2061–2068.
[47] A. Ceulemans, L.G. Vanquickenborne, J. Am. Chem. Soc. 103 (1981) 2238–2241.
[48] E.M. Kober, T.J. Meyer, Inorg. Chem. 21 (1982) 3967–3977.